

| | | |
|--|------------------------------|--|
| <small>PAUL SCHERRER INSTITUT</small>  | <h1>HESSI</h1> | Document Identification HESSI-HR34-005 |
| Laboratory for Astrophysics | Contamination Control | PKS-Code: =6 TGA 20 |
| DocTyp: <input type="checkbox"/> Management <input type="checkbox"/> Product | Document_Typ_Name | Issue: 20.06.1998 Update: 10.11.2000 |

HESSI Contamination Control

Scope of the document

The document describes the issue of contamination control for the HESSI instrument.

HSI_SYS_039B

Distribution:

| Expl. Name | Expl. Name |
|------------|------------|
| | |

Prepared by: Dr. R. Henneck Signature _____ Date _____
 Name _____

Approved by: Dr. A. Zehnder Signature _____ Date _____
 Name _____

| | |
|--|------------------------------------|
| Depository: <input type="checkbox"/> A. Zehnder <input type="checkbox"/> ODRA/120 <input type="checkbox"/> P. Ming OTLA/110 <input type="checkbox"/> | Remarks: Foreign ID: |
|--|------------------------------------|

1. Background

Contamination comes essentially in two kinds:

- Films of ‘molecular’ contaminants (mostly hydro-carbons, silicones and combinations thereof) of a more or less uniform thickness. Affects the transmissivity by **absorption**.
- Particle contamination (‘dust’). Affects the transmissivity by **absorption and scattering**.

Dust is a major concern on **surfaces close to the CCD**, e.g. on the CCD glass window, since there a dust grain of 20 μ may completely obscure one pixel or fake some funny Sun limb structure.

1.1. Estimation of contaminant production

This is rather difficult to predict since it depends on the cleanliness measure taken and is therefore not easily comparable from spacecraft to spacecraft. Rough values for molecular films for the SCATHA mission predict something like 0.3 $\mu\text{g}/\text{cm}^2$ after 1 year in the Sun shadow but about **3 mg/cm^2 for Sunlit surfaces** (see Fig.1a).

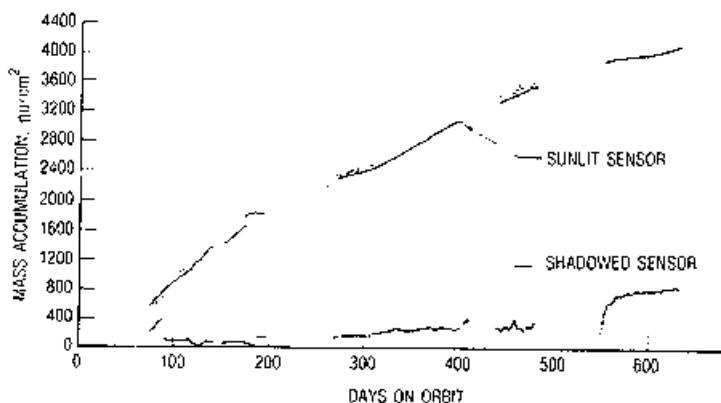


Fig. 1a Mass Accumulation on the SCATHA ML-12 Temperature Controlled Quartz Crystal Microbalances

The UV-stimulated mechanism for enhanced deposition is well documented and has been verified in the laboratory. It is based on ionization of ambient molecules and their subsequent attraction to nearby surfaces. In general the Sun reflected Earth albedo contains relatively little hard UV as compared to the direct Sunlight and no evidence for such stimulated contamination has appeared in the literature until recently. However, on the HST WFC-1 some excessive contamination was found which was explained on the basis of UV stimulated polymerization [3]. Thus, some care should also be taken for the RAS which sees the Sunlit Earth for about 20% of its time.

1.1.1. Potential cleaning mechanisms

Molecular films (except for silicones) are removed under the impact of atomic oxygen (AO) at velocities corresponding to about 5 eV. Solid hydrocarbons are thus transformed into volatile reaction products. This has been shown to clean optical surfaces with the onset of solar activity when the density of AO increases by 2 orders of magnitudes. Several instruments (visible) on NIMBUS 6, 7 which look into the ram direction have experienced complete transmission recovery in the course of 1978

([7], see Fig. 2). 100 times higher AO densities are expected for HESSI, since it flies at an altitude of only 600 km while NIMBUS 6, 7 were flying at 1100 km and 960 km respectively. However, the cleaning effect depends on the fraction of time the SAS/RAS looks into the ram direction. This is about 20% for the SAS and about 10% for the RAS; hence it appears difficult to quantify the net cleaning effect.

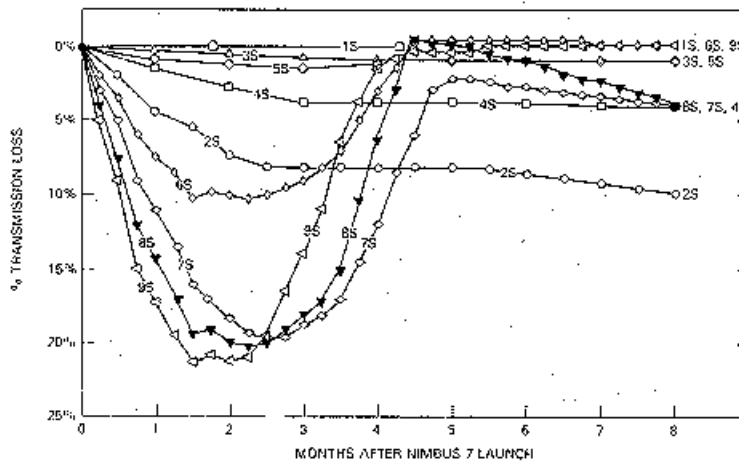


Fig. 2: Transmission loss and recovery of all ERB solar channels on Nimbus 7 during the first 8 months [7].

1.2. Estimate of contaminant effects

1.2.1. Molecular films

The absorption effect of molecular films can be estimated as follows:

$$I = I_0 e^{-\alpha t} \quad \text{with}$$

I = transmitted intensity

I_0 = incoming intensity

t = thickness of contaminant layer [μ]

α = absorption coefficient [μ^{-1}]

α is a function of contaminant composition and wavelength and is unfortunately only badly characterized. Fig.3 shows results for space-relevant contaminants from Refs.[1],[4],[6]. Table 1 shows typical film thicknesses for a transmission loss of $1/e$ at various wavelengths in the visible with upper/lower bounds given by the range in α .

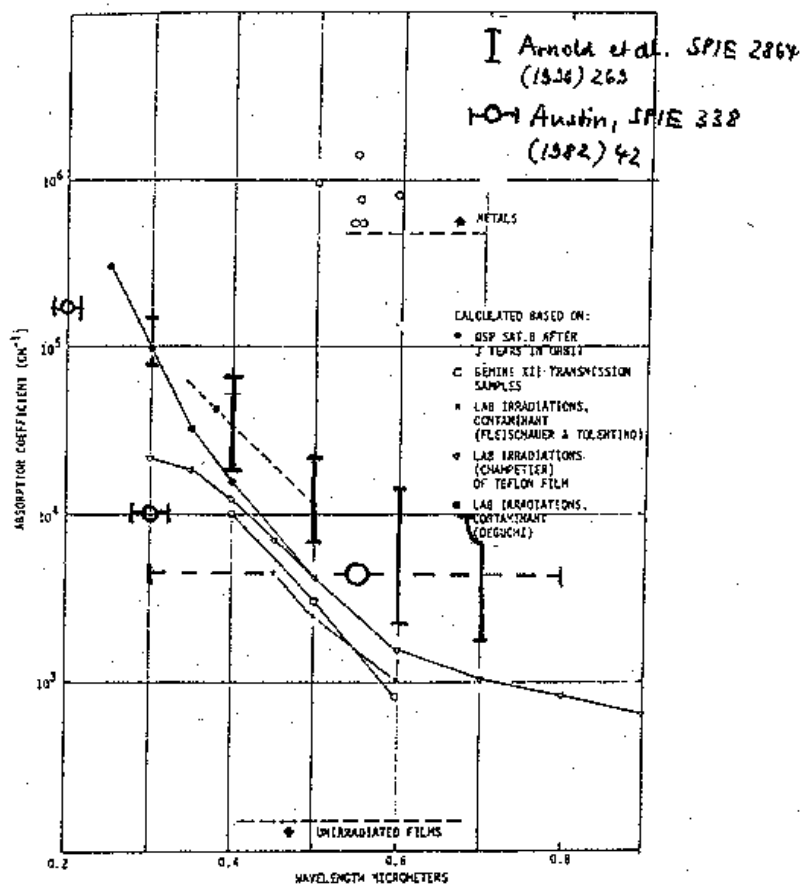


Fig.3: absorption coefficient α from Refs.[1],[4],[6].

Under the hard solar UV radiation ($\lambda < 250$ nm) the hydrocarbon bonds get cracked ('solarization', 'photopolymerization', 'photolization') and the deposit changes toward a darker color and becomes much more tenacious. Using α for 'glassy carbon' [2] one obtains roughly 20x higher absorption e.g. at 700 nm for the same thickness, see Table 1.

Table 1: absorption coefficient α and $1/e$ film thickness ($I/I_0 = 1/e$) versus wavelength for hydro-carbons (HC) and glassy carbon (GC) [2].

| | 300 nm | 400 nm | 500 nm | 700 nm |
|-----------------------------------|----------|----------|-----------|------------|
| a [m^{-1}] HC | 1 - 15 | 0.5 - 7 | 0.3 - 3.3 | 0.05 - 1 |
| a [m^{-1}] GC & | 30 | | 17.7 | 13.5 |
| $1/e$ thickness[m] HC | 0.07 - 1 | 0.14 - 2 | 0.3 - 3.3 | 1 - 20 |
| $1/e$ thickness[m] GC & | 0.033 | | 0.057 | 0.074 |
| $1/e$ thickness[mg/cm^2] HC * | 7 - 100 | 14 - 200 | 30 - 330 | 100 - 2000 |
| $1/e$ thickness[mg/cm^2] GC* | 3.3 | | 5.7 | 7.4 |

* with $\rho = 1$ g/cm³

& from Ref.[2]

1.2.2. Particles

Settled particles are measured in terms of their equivalent quantity in accordance with the particle levels given by MIL-STD-1246A (not to be confounded with “air class A”). Table 2 lists approximate values of surface coverage or obscuration as a function of settled particle levels [5]. The assumption was made that all particles were spherical and they did not overlap. Thus these obscuration values probably represent a worst case because these assumptions are not true for real settled particle distributions. “**Just visible clean**” corresponds to level **500 to 750**.

Table 2: Approximate surface obscuration versus particle coverage level

| Particle level | Obscuration [%] | Particle concentration >5m [n/cm ²] | Particle concentration >25m [n/cm ²] | No. particles >5m on SAS CCD | No. particles >5m on RAS CCD |
|----------------|-----------------|---|--|------------------------------|------------------------------|
| 100 | .00027 | 1.9 | .084 | 0.006 | 0.25 |
| 200 | .0045 | 30 | .133 | 0.1 | 3.9 |
| 300 | .03 | 183 | 8 | 0.6 | 23 |
| 400 | .11 | 707 | 31 | 2.4 | 82 |
| 500 | .32 | 2110 | 93 | 7 | 238 |
| 600 | .80 | 5330 | 234 | 18 | 612 |
| 700 | 1.8 | 11900 | 522 | 40 | 1360 |
| 800 | 3.6 | 24200 | 1060 | 82 | 2788 |

The settling of particles onto surfaces is controlled primarily by controlling the local air-borne particle distribution (clean rooms, clean garments, covers, bags). For particles over 5 – 10 μ in diameter relatively high turbulent air velocities are required to transport them into a covered volume. Therefore for ground operations, a simple cover over the top and sides of an item can protect it from airborne particles if turbulence is prevented around the bottom or skirt of the cover. Preferably, however, the cover would fully enclose the item.

Connection between ‘particle level’, air-class A (standard definition: No. of particles > 0.5 μ /ft³) and exposure times is made in Table 3 [5]. The No. of particles >5 μ /ft³ is approximately given by

$$N(>5 \mu) \approx 0.0063 * A.$$

Thus, in a clean bag filled with cleanroom air, there is relatively few particles. The problem is fallout of particles with exposure time.

Table 3:

| | Exposure time [d] for level 300 (100) | | | |
|-----------|---------------------------------------|-------------|------------------------|------------|
| | Normal cleanroom | | Laminar flow cleanroom | |
| Air-class | horizontal | vertical | horizontal | vertical |
| 100 | 20 (0.34) | >200 (2) | 110 (1) | >200 (13) |
| 500 | 0.08 (<<0.1) | 0.7 (<<0.1) | 0.35 (<<0.1) | 4.5 (0.05) |
| 1000 | << 0.1 | <0.1 | <<0.1 | <0.1 |

2. HESSI contamination budget

Table 4 gives the contamination budget, which is obtained when all open surfaces are allowed to be contaminated. Concerning particle contamination the RAS and SAS are very critical with respect to particles sitting directly on the CCD window. Following Table 2 we would like to have **medium-low settled particle levels (<600)** which in terms of obscuration have a negligible contribution to the overall degradation.

Table 4:

| system | Particle density on CCD [level] | Allowable transmission after 2 y [%] | Allowable molecular contaminant [mg/cm ²] | Expected molecular contamination [mg/cm ²] |
|-----------------------|---------------------------------|--------------------------------------|---|--|
| SAS & (front surface) | 600 | 5 | 21 & | ≥ 3.5 |
| RAS * (3 surfaces) | 600 | 50 * | 140 * | ≥ 1 |
| RAS & (front surface) | 600 | 60 | 4 & | ≥ 0.23 |

* neglecting UV solarization effects.

& effect of completely UV/AO polymerized contaminant on lens front surface only, $\alpha = 14 \mu^{-1}$ and $\rho = 1 \text{ g/cm}^3$

3. General cleanliness measures

Cleanliness measures to be followed for HESSI:

1. Cleanroom handling on ground (class 1000 for CCD handling, class 100000 for optical systems)
2. Space-qualified only materials selection
3. Optimize venting geometries, e.g. no venting of MLI onto optics
4. Cold 'baffling': reduce direct view-factors to outgassing surfaces and reduce sticking on optics
5. nitrogen purging and nitrogen environment up to launch
6. baking of MLI
7. cleaning of lenses at the last possible moment

References:

- [1] G.S. Arnold, K. Lucy, 'Photochemically deposited contaminant film effects', SPIE Vol. 2864 (1996), 269
- [2] M.W. Williams, E.T. Arakawa, 'Optical properties of glassy carbon from 0 to 82 eV', J. Appl. Phys. 43, 3460 (1972)

[3] J.T. Tveekrem et al, 'Contamination-induced degradation of optics exposed to the Hubble Space Telescope interior', SPIE Vol. 2864 (1996), 246

[4] J.A. Austin, 'Contamination control plan for prelaunch operations', SPIE Vol. 338 (1982), 42.

[5] J.D. Buch, M.K. Barsh, "Analysis of particulate contamination buildup on surfaces", SPIE Vol.777 (1987), 43

[6] M.E. Frink, M.A Folkman, L.A Darnton, 'Evaluation of the UV/ ozon technique for on-orbit removal of photolyzed molecular contamination from optical surfaces', SPIE Vol. 1754 (1992), 286.

[7] R.E. Predmore, H. Jacobowitz, J.R. Hickey, 'Exospheric cleaning of the Earth radiation budget solar radiometer during solar maximum', SPIE Vol. 338 (1982), 104.

HESSI SAS and RAS lens contamination

Based on the document **HESSI Contamination Control** from 20.6.1998 (called Ref.1 in the following), it was evident that the contamination issue is of importance and all possible standard, simple cleanliness precautions were executed during integration and ground operations, including a pre-bakeout of the MLI and of the cables. However, HESSI is not using gas propellents, the CCD wavelength ranges (400 to 1000 nm) are not especially critical for contamination and, in general, optical baffles are also quite effective against residual gas components around. Given the safety factors which can be applied, no highly-elaborate, time- and resource-consuming procedures were thought to be necessary. The conclusions from this note are with respect to a mission duration of 2 years. The following note addresses in more detail a potential degradation of the SAS / RAS optical performance due to **absorptive films of contaminants** (mostly hydro-carbons, silicons and combinations thereof). Pure contamination layers are of less concern, since they are almost transparent (we have used an absorption coefficient of $0.5 \mu^{-1}$ around 400nm [1]). However, under the influence of UV photons (≤ 200 nm) and /or atomic Oxygen (AO) the probability for sticking is strongly enhanced and polymerization may take place. It should be noted however, that AO also has a cleaning effect (see below). The general rule-of-thumb is that silicones are preferentially deposited under AO bombardment while carbonic matter is removed. Polymerization also changes the absorption coefficient (we have used the upper limit at 670 nm of $2 \mu^{-1}$ [1]) and thus the transmissivity. Please note, that the conclusions of Ref.1 were derived by using the much higher absorption coefficient for glassy carbon ($14 \mu^{-1}$) which was at that time recommended to us by the ESA contamination control group [2].

Particulate contamination is of influence only on surfaces close to the foci of the systems which are all inside the sealed electronic CCD housings. Microscope inspection of all 3 SAS CCD windows after the vibration mishap showed essentially no dust particles, similar to pre-vibration conditions. Information on this specific problem is discussed in Ref.1 and will not be discussed here.

4. SAS

4.1. Tolerance limit

Based on the numerous Sun observations we did on ground with the FM imager, standard operation will need CCD integration times in space of around 400 μ s. In case of lens darkening we can adapt the integration time of each SAS individually in steps of 16 μ s up to 2 ms without performance loss, resulting in a safety factor of 5.

Standard operation foresees pixel amplitudes for maximum Sun irradiation close to saturation, i.e. about 900 ch, with the limb defining threshold at about 30%. Since the CCD dark current is ≤ 25 ch even for 2 ms, we can also operate with negligible loss of aspect accuracy when the maximum response is only about 220 ch (and even lower if we can tolerate loss of aspect accuracy). Combined with the above we can thus **allow a lens darkening factor of at least 20**.

No attempt was made to estimate the amount of outgassing, also because even elaborate modelling yields deposition predictions which typically vary by an order of magnitude (as e.g. demonstrated for the Environmental Verification Experiment [3]). Comparison between measured contamination effects in space should be viewed with caution, since they depend very sensitively on the geometry, materials, temperature, contamination control executed, wavelengths, space environment, orbit, potential cleaning mechanisms etc. Even "deposition predictions typically vary to an order of magnitude" [3], the more so, if one wants to compare one spacecraft to another. Therefore, an **uncertainty factor of 20** is applicable if we want to derive HESSI deposition limits on the basis of other spacecraft experience. For permanently sunlit surfaces, virtually no degradation has been observed for TRACE and for MDI on SOHO [4]. Clearly, contamination control for these 2 missions was much more strict. The SCATHA mission (Fig.1a of Ref.1) gives a mass accumulation of about $4.4 \mu\text{g}/\text{cm}^2$ after 2 years for a **sunlit** sensor. Taking into account that HESSI is in the Earth-shadow for 1/3 of its orbit, this would yield a deposition of $3.5 \mu\text{g}/\text{cm}^2$ and a lens transmissivity of 0.93. SCATHA was launched in 1979 during Solar max into a HEO, where no AO cleaning would happen. Note also, that about 30% of the SCATHA contamination was deposited during periods of plasma spacecraft charging in connection with UV illumination, an effect specific to the high plasma densities at HEO [1]. Thus, even if it was probably a cleaner mission, it should be representative for HESSI.

4.2. Measures to reduce contamination

Fig.1 shows the SAS front lens surroundings. The lens is made from fused Silica (Infrasil) with a lower wavelength cutoff around 230 nm and does not transmit the most dangerous UV below 200 nm. The lens' outer, convex surface is coated with a standard anti-reflective coating while the flat backside carries the bandpass-defining, hard, ion-plated film. This coating is 100% reflective over the range 500 nm to 900 nm (with the exception of the narrow bandpass at 670 nm) and transparent elsewhere. The heating due to the Sun absorption on the polished Al aperture ring results in a thermal input on the lens support of 0.2 W. Given the very good thermal contact and an anticipated temperature of the front tray of about 20° C we calculated the temperature of the lens to be the same as for the tray.

The temperature of the lens baffle results from the balance between the heat input from diffuse reflection from the lens aperture ring (note, that specular Sun reflection from the lens cannot reach the baffle insides during normal HESSI operation with a pointing range of 1°) and radiative cooling due to the special foil applied to the baffle outsides (silver-coated Teflon, with $\alpha \sim 0.1$ and high $\epsilon \sim 0.9$). The baffle is thermally isolated from the CFRP scaffold. We calculated the baffle temperature to be about 15° C lower than the lens/ tray temperature (at the nominal 20° C) for the most unfavorable case when the baffles are exposed to Earth-reflected Sunlight over 40% of their surface. It was found to be slightly colder for the case when HESSI is in the Earth shadow. Thus, the SAS baffles will work as cold barrier for **external** contaminants.

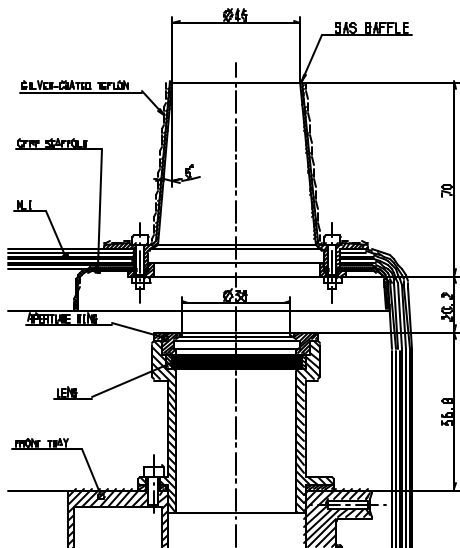


Fig.1: SAS front lens and surroundings

5. RAS

5.1. Tolerance limit

Here the tolerance limit is much tighter; the RAS sensitivity cannot be reduced by more than a factor 2 since the minimum number of stars detected is a very steep function of sensitivity.

Limits on the expected contamination can again be derived from the SCATHA results: the SAS is estimated to pick up $3.5 \mu\text{g}/\text{cm}^2$ after 2 y (see above). Assuming that the RAS sees the earth for only 20% of its observation time and the earth-reflected UV is reduced by a factor of 3 then we obtain $0.23 \mu\text{g}/\text{cm}^2$ contaminant and a transmissivity reduction of 0.5% (using $1\text{g}/\text{cm}^3$ density and an absorption coefficient of $2 \mu^{-1}$). Given the tolerance limit quoted above this yields a safety factor of 150 for contaminant thickness increase.

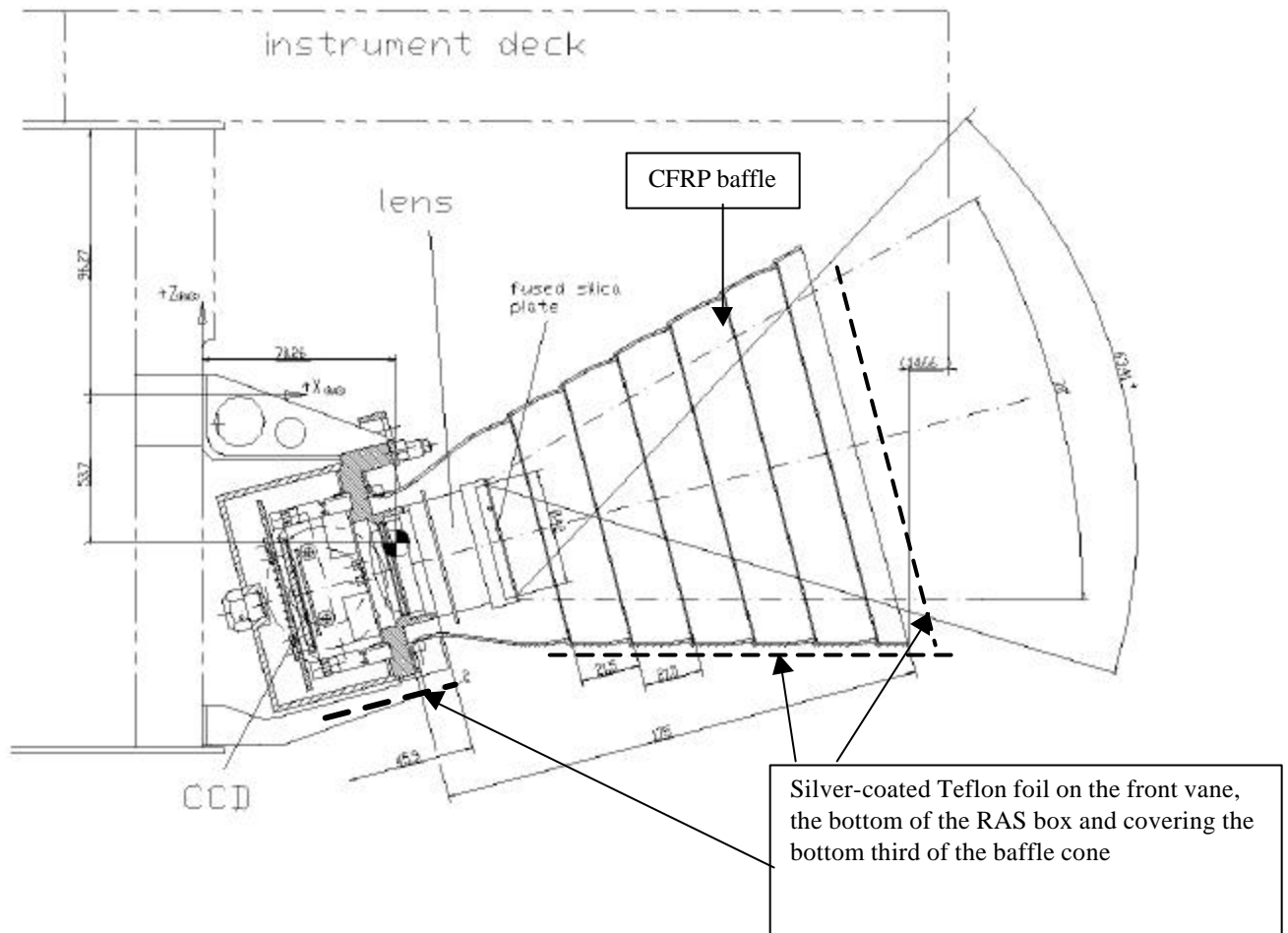


Fig. 2: Cross section of the RAS. The z-axis is pointing towards the Sun.

5.2. Measures to reduce contamination

Fig.2 shows the RAS geometry. The lens is a commercial Leica Summilux, f/1.4, 50 which was assembled oil-free and using space-qualified adhesives. A 4 mm thick fused silica plate in front of the first lens serves for radiation protection. The thermal properties of the FM system were measured in the PSI 'cold space' simulation chamber for typical heat loads of the CCD and front-end electronics (1.5 W). Specifically, the temperatures were measured on the baffle front vane and close to the baffle support. The baffle front temperature was found to be colder than the lens temperature by 2°C up to 9°C , depending on whether we assumed a warm ($+40^\circ\text{C}$) or

a cold (-20°C) spacecraft and RAS switched on or off. The most probable case of a 20°C warm spacecraft and RAS on yields about 7°C difference. The effective thermal conductivity of the composite baffle along the cone direction was evaluated to be about 200 W/m/K, i.e. similar to that of Al. Thus, again, the baffle temperature is lower than the front surface exposed to contamination.

6. Cleaning mechanisms / Atomic Oxygen

Cleaning mechanisms are due to the impact of energetic (≥ 5 eV) AO and - on a less well documented level - energetic atomic H and/or O^+ , H^+ impinging on the contaminated surfaces with high velocity. The effect is selective however [5]: it works very well for CFRP and acrylic adhesives (almost complete removal of contamination, both exposed and unexposed to UV at the same time) and partially for conformal coatings (Solithane 113) and polyurethane-type compounds. Contrary to the examples given in Fig.3 of Ref.1, HESSI will fly at about 600 km altitude, always during Solar maximum, which yields an AO concentration higher by 2 orders of magnitude. The much higher concentration should offset the effect that the SAS looks only about 20% of its time into the ram direction and the RAS about 10%. Since CFRP is for the RAS the by far dominant close-by contamination source, and for the SAS the main contributor due to partial vacuum venting via the baffle holes, a significant cleaning effect can be expected which is however difficult to quantify.

The front surfaces of both systems – SAS and RAS – are covered by anti-reflective coatings with a SiO₂ top layer. SiO₂ is known to be immune to AO for thickness layers ≥ 4.5 nm [6] and protects the underlying layers.

7. Internal surfaces which are inside the MLI enclosure or within the CCD housings

These surfaces are subject to contamination from internal sources only, which is probably higher than for external surfaces. However, due to the absence of the UV component and AO there is no induced layer increase / blackening. This allows a buildup of much thicker coatings than for external surfaces and is hence considered to be negligible.

8. PEGASUS launch failure

In case the PEGASUS launch has to be interrupted in flight, it could happen that the cold optical surfaces would acquire condensation water upon return to ground. If the re-start would take place within a short time without removal of the condensation water, it would freeze in-flight. The SAS lens/tray temperature will never fall below 0°C in-flight, however the RAS operating temperature will be below 0°C and the potential ice on the lens will only slowly sublimate. To avoid this the RAS lens is purged from fairing closeout through takeoff by dry Nitrogen.

9. Conclusions

Conclusions given in Table 1 are for 2 years in orbit. For the ‘expected molecular contamination’ and the ‘thickness safety factor’ we have quoted limits, where the low contamination limit derives from the SCATHA results discussed above. For the high contamination limit we have multiplied these numbers by an **uncertainty factor of 20**. This is applicable since even “deposition predictions typically vary to an order of magnitude” [1] and the more so, if one wants to compare one spacecraft to another without detailed knowledge of geometry, materials, temperatures, contamination control executed, wavelengths, space environment, orbit, potential cleaning mechanisms etc.

For the RAS we also present the case when no induced polymerization should take place and only contamination of the relevant 3 surfaces (CCD window, lens front and back surface) is considered, using the SCATHA results for a ‘**shadowed**’ sensor.

Table 1: HESSI molecular contamination budget summary

| system | Allowable min. lens transmission [%] | Allowable molecular contaminant [mg/cm ²] | Expected molecular contamination [mg/cm ²] | Thickness safety factor |
|-----------------------|--------------------------------------|---|--|-------------------------|
| SAS & (front surface) | 5 | 150 ^{&} | 3.5 70 | 2 ... 43 |

| | | | | |
|-----------------------|------|-------|---------------|------------|
| RAS * (3 surfaces) | 50 * | 140 * | 1 20 | 7 ... 140 |
| RAS & (front surface) | 50 | 35 & | 0.23 4.6 | 7 150 |

* neglecting UV/AO polymerization effects.

& effect of UV/AO polymerized contaminants on lens front surface only, absorption coefficient $2 \mu^{-1}$ and $\rho = 1 \text{ g/cm}^3$.

References

- [1] NASA Contractor Report 4740, A.C. Tribble et al. 'Contamination Control Engineering Design Guidelines for the Aerospace Community' (1996).
- [2] M. Van Eesbeek, private communication
- [3] <http://watt-a-server.gsfc.nasa.gov/Groups/p2/projects/eveep/eveep.htm>
- [4] T. Tarbell, Lockheed-Martin, private communication
- [5] Y. Noter et al, „Variations in the Telemetry of an OFFEQ Satellite’s Sun Sensors“, 7th International ESA Symposium on 'Materials in Space Environment', Toulouse, France, June 1997, p.143-152.
- [6] M. Tagawa et al, „Oxidation of Room Temperature Silicon (001) Surfaces in a Hyperthermal Atomic Oxygen Beam“, 7th International ESA Symposium on 'Materials in Space Environment', Toulouse, France, June 1997, p.225 - 229.